

# Multiple windows algorithm for event detection in STFT-BOTDR

Yifei Yu<sup>1</sup>, Linqing Luo<sup>1</sup>, Bo Li<sup>1</sup>, Jize Yan<sup>1,2\*</sup> and Kenichi Soga<sup>1</sup>

*<sup>1</sup> Department of Engineering, University of Cambridge, Trumpington Street, Cambridge, CB2 1PZ, UK*

*<sup>2</sup> Electronics and Computer Science, University of Southampton, Southampton, SO17 1BJ*

*\*Corresponding author: yanjize@gmail.com*

**ABSTRACT** Short-time Fourier Transform (STFT) as a class of the time-frequency analysis have been utilised to deliver a fast-speed, accurate and low-variation BOTDR (Brillouin Optical Time Domain Reflectometer) system. The different window functions applied in the signal processing are important to improve the spatial resolution, frequency resolution, and variance of the BOTDR and to detect small event in the real application such as strain or temperature events smaller than the pulse length along the fibre. Window functions with long duration can achieve high frequency resolution, but be difficult to detect events less than the window length. While, small-length window offers better event detection performance than the long-duration window, but induces high variation along the fibre under test (FUT). For instance, the rectangular window offers a better frequency resolution; and the hamming window is better at the event detection. This paper introduces an optimised algorithm by utilising two separate windows and comparing the Brillouin frequency difference along the distance domain between the results generated by different windows to enhance the capability of small event detection, such as cracks and sharp temperature variation along the fibre.

## 1. INTRODUCTION

Distributed optical fibre sensors based on Brillouin scattering have attracted significant interest for diagnosing deterioration and preventing disasters in the field of health monitoring for large civil structures, such as pipe lines, bridges, tunnels and dams in the past few decades (Bao and Chen 2011; Lee 2003). BOTDRs (Brillouin Optical Time Domain Reflectometers) have been utilised to measure the distributed strain and temperature along the entire optical fibre by monitoring the Brillouin Frequency Shift (BFS) of the scattering. In the BOTDR system, a laser probing pulse is launched into the sensing fibre under test (FUT) and its Spontaneous Brillouin Scattering (SpBS) spectrum along the fibre is measured at the same end of the fibre, which is convenient for the field applications (Horiguchi et al. 1995; Bergman, and Tur 2015). The conventional BOTDR system demands a time consuming frequency scanning of the entire SpBS spectrum and a great amount of averaging up to  $2^{20}$  times to acquire the accurate Brillouin scattering spectrum (BSS) (Ohno et al. 2001; Wang et al. 2009).

Recently, a fast-speed Discrete Fourier Transform (DFT)-based BOTDR has applied the wideband detection architecture accelerated by a Digital Signal Processing (DSP) and/or Field Programmable Gate Array (FPGA) to replace the time-consuming frequency sweeping method, moreover, it takes only 1 s to measure the frequency-down-converted SpBS signal up to 500 MHz over the 1.5 km testing fibre (Ohno et al.

2001; Lu et al. 2008). This wideband detection has been demonstrated at a temperature resolution of 3 °C and a spatial resolution of 2 m for 6 km fibre (Lu, Dou, and Zhang 2008). Very recently, the zero-padding enhanced STFT-BOTDR has been demonstrated, which offers an analysis on the spectrum deformation of the BOTDR system to improve measured distance accuracy (Yu et al. 2015). In Short-Time Fourier Transform (STFT) BOTDR system, a short duration window is applied to achieve a better spatial resolution, which will worsen the frequency resolution of SpBS. In contrast, a longer window would improve the frequency resolution but reduce the spatial resolution. In real applications, the frequency resolution of the SpBS determines the strain and temperature resolution, and the spatial resolution is essential for the strain or temperature events smaller than the pulse length detection.

This paper applied the zero-padding-enhanced STFT method to a temperature measurement of different length of fibre, for demonstrating the influence of the window type and duration to the BOTDR system to compare the spatial resolution, frequency resolution, variance and short-length event detection. The highest spatial resolution of the STFT-BOTDR is determined by the probe pulse length, which severely influenced by the number of data in each frame of STFT and linearly increases with increasing window size (Horiguchi et al. 1995; Wang et al. 2009). Accordingly, an event with length smaller than the pulse duration or the window length is not detectable, including the actual length and Brillouin frequency shift. In other

words, a detectable event must contain a length larger than both of the pulse duration and window length in order to offer an undamaged Brillouin frequency shift and length. To overstep the uncertainty principle between frequency and time resolution of the STFT method (Flandrin, Lin, and McLaughlin 2013), a combination of variant window types and durations algorithm has been proposed in this paper to deliver a comprehensive result. Based on the Brillouin frequency difference along the distance between two windows, the smaller-length event and Brillouin frequency transition region can be worked out. According to this indication, an optimised result from multiple windows can be achieved.

## 2. THEORY

Time-frequency distributions are designed to characterise the time-frequency content of signals. STFT is a linear time-frequency transform applied to evaluate the frequency and phase content of local sections of a signal as it changes over time (Hlawatsch and Francois 2008). The back-scattered Brillouin signal captured by the digitiser of a coherent heterodyne BOTDR system can be represented as discrete frequency domain information (Geng et al. 2007). In the case of a wideband receiver, the data to be transformed need to be split up into frames and each frame is Fourier transformed for observing localised spectrum of a signal. The discrete STFT can be represented by (Hlawatsch and Francois 2008):

(1)

where  $x[n]$  is the signal to be transformed, and  $w[n]$  is the window function. The window duration and type are the two important variables in the STFT process. DFT requires the signal length to be finite in each frame, which means the N-point DFT operates on an N-elements data vector  $x[n]$  to produce an N-element result in a frequency domain  $X[K]$  (Durak and Arikan 2003).

$$X[k] = \sum_{n=0}^{N-1} x[n] e^{-j2\pi nk/N} \quad (2)$$

Since the frequency resolution is inversely proportional to the analysing window duration, it is difficult to ensure a good stationarity and good frequency resolution at the same time (Abdelghani and Fethi 2000). It is suggested to keep the duration of the sliding window as short as possible to ensure the stability, but reducing the frequency resolution of the spectrogram (Abdelghani and Fethi 2000), which is known as Heisenberg uncertainty principle (Busch, Heinonen, and Lahti 2007) and a time and frequency resolution trade-off to be considered.

The various types of window can be utilised in signal with different characteristics. The rectangular window can be used to truncate the data

sequence, while the other windows such as hamming, Gaussian and Blackman windows offer some data weighting (Harris 1978). The advantage of applying a window other than rectangular is to have lower sidelobes. However the disadvantage is a loss in frequency resolution (Hlawatsch and Francois 2008). If the actual signal length  $L$  is less than  $N$ , the data vector can be extended by “zero-padding” which accounts to putting zeros at the end of digitised time domain signal (Hlawatsch and Francois 2008). The advantages of zero padding and the corresponding peak-searching method applied in the STFT-BOTDR system are more immune to Brillouin spectrum deformation and asymmetry (Yu et al. 2015).

The minimum detectable frequency shift is a function of the Full Width at Half Maximum (FWHM) and Signal to Noise Ratio (SNR) in the BOTDR system (Horiguchi et al. 1995), which is given by:

(3)

## 3. EXPERIMENTAL RESULTS AND DISCUSSION

The FUT setup can be represented by Figure 1. The total FUT consists of nine sections of single mode fibre (SMF) controlled by a water bath during the experiment. The interval between the temperature controlled sections is 10 m. The temperature was set to be stable at 75 °C.

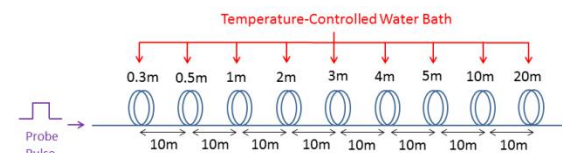


**Figure 1.** Experimental setup for the temperature-controlled unit of the STFT-based BOTDR system.

Fig. 2 illustrates the schematic representation of the STFT-BOTDR system with temperature calibration unit. Branch A and B were split by a 90/10 coupler from a continuous-wave laser diode. The branch A was modulated by an Electro-Optical Modulator (EOM) with 34 ns modulating pulse, amplified by an Erbium-Doped Fibre Amplifier (EDFA). The amplified pulse light went through an optical filter followed by a circulator, and then launched into a 1.5 km FUT. The branch B is regarded as a reference light connected by a polarization scrambler (PS) and utilised as an optical local oscillator (OLO). The branch B mixed with the backscattering light via a coupler and a 26 GHz photodetector (PD) for coherent detection. The down-converted signal was captured by a 5 GS/s digitiser.

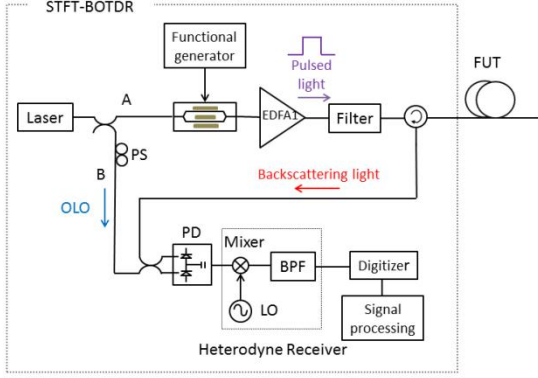


**Figure 2.** Experimental setup for STFT-BOTDR. PS, polarization scrambler; EDFA, erbium-doped fibre amplifier; EOM, electro-optic modulator; FUT, fibre under test; OLO, optical local oscillator.

### 3.1 Window type

Five types of window have been applied to the STFT-BOTDR system, including Hamming, Gaussian, Rectangular, Blackman and Chebyshev window. With fixed window duration, readout and zero-padding, the measured Brillouin centre frequency along the distance axis is displayed in Fig. 3. It is observed that the variations along the distance axis for five windows are different. The variation for the rectangular window is 3.98 MHz, which is the lowest among these five windows. Moreover, the rectangular window brings the most rapid frequency transition region shown in Fig. 4, which can be regarded as the shortest detectable event length. The spatial resolution for the rectangular window is 2m. Moreover, the FWHM measured for these five kinds of windows in the same position is illustrated in Fig. 6. The rectangular window can offer lowest FWHM, so that the measured frequency resolution is the best in this window measurement. However, the rectangular window can not detect the event, of which the length is less than the pulse duation indicated in Fig. 5.

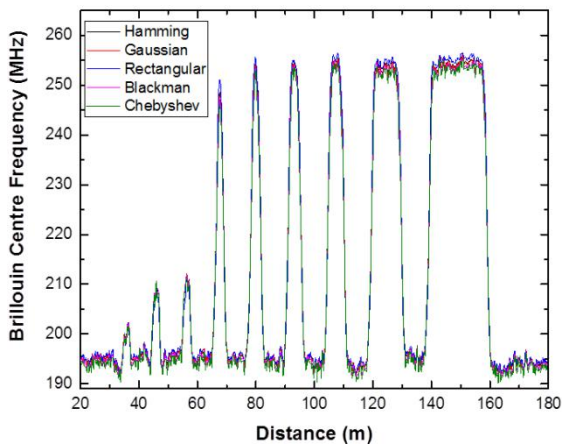


**Figure 3.** Experimental results of Brillouin centre frequency for 75°C temperature test with different window types.

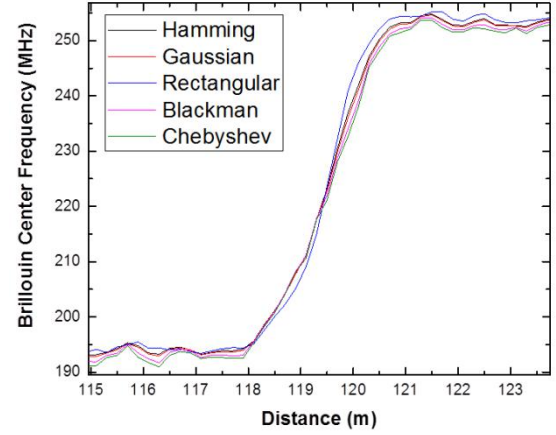


**Figure 4.** Experimental results of Brillouin centre frequency for 75°C temperature test with different window types in the frequency transition region.

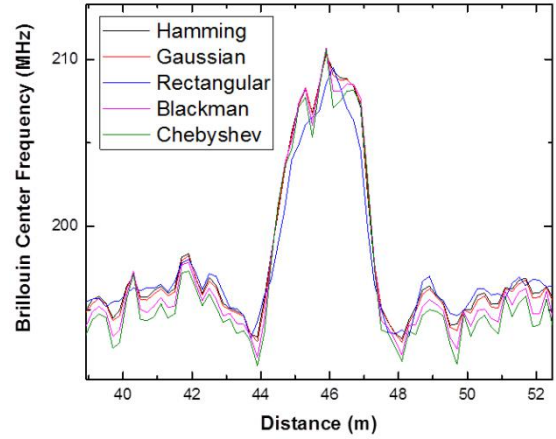


**Figure 5.** Experimental results of Brillouin centre frequency for 75°C temperature test with different window types in the 0.5m section.

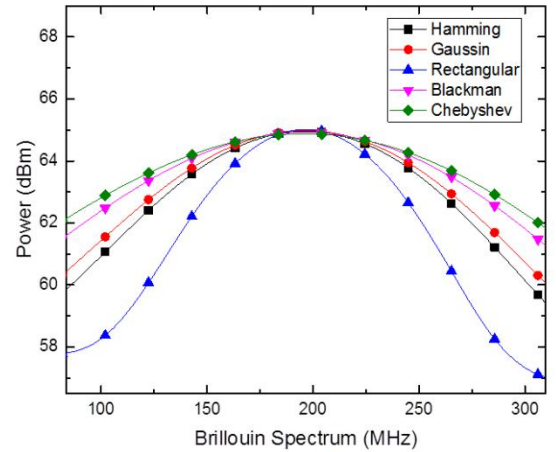


**Figure 6.** Experimental results of the Brillouin spectrum in a same position for the five types of windows.

The reason for these results is due to both of the characteristics of window functions and STFT-BOTDR system algorithm. The rectangular window has excellent resolution characteristics for sinusoids of comparable amplitude, but it is a poor

choice for sinusoids of disparate strength (Harris 1978). Furthermore, rectangular window offers best frequency resolution. The major limitation of using rectangular window is high side lobes in the frequency domain. But due to averaging process and Gaussian fitting, only the three peak points are utilised to find the Brillouin peak location, the high sidelobes effects can be minimised. The back scattering signal cannot be distinguished within half pulse length, which leads to limitation of spatial resolution to be the pulse length (Wang et al. 2009). The usage of rectangular window equals to truncate these data without any weighting. Because the hamming window changes the weight of each frame in DFT, the centre data contribute more than the fringe data (Wang et al. 2009). The hamming window shows good detection performance in the events less than the pulse length, because the window is optimised to minimise the nearest side lobe. In this case, it is observed that a window with high main lobe to side lobe ratio is capable to strain or temperature events smaller than the pulse length detection, such as hamming window. In the STFT-BOTDR system, a hamming window is good at less than pulse length detection, such as cracks; a rectangular window is recommended to be applied for low variation, high spatial resolution and frequency resolution.

### 3.2 Window size

Window size is crucial in the STFT-BOTDR signal processing. A long window brings high frequency resolution, but low time resolution. This equals to good strain/temperature resolution and bad spatial resolution in the BOTDR system. Moreover, low FWHM is generated by a long window, which means high frequency resolution is provided. A short window leads to high time resolution but coarse frequency resolution. This kind of window is good at detecting the event less than the pulse length. There are four durations of windows applied in the STFT process of the BOTDR system. It is observed that the lowest variation (2.48 MHz) along the distance is obtained by the window with 40 ns duration displayed in Fig. 7. This relatively long window can also bring the shortest detectable event length (0.4 m) shown in Fig. 8. Additionally, the FWHM for the 40 ns duration window is the lowest among these four windows illustrated in Fig. 10, which indicates the highest frequency

resolution. The long window is not good at 0.5 m event detection displayed in Fig. 9. The shortest window (10 ns) is more sensitive to the event with length less than the duration of the probe pulse.

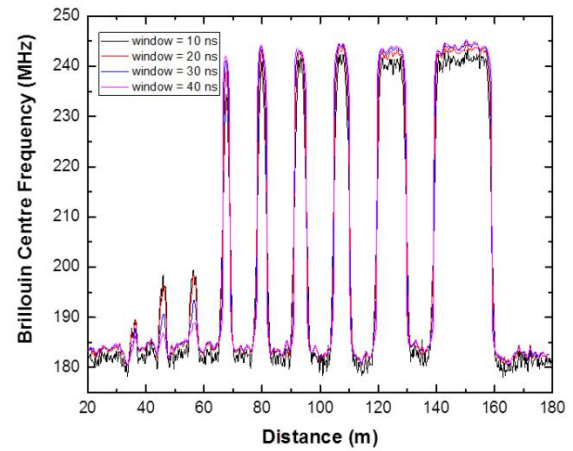


**Figure 7.** Experimental results of Brillouin centre frequency for 75°C temperature test with different window durations.

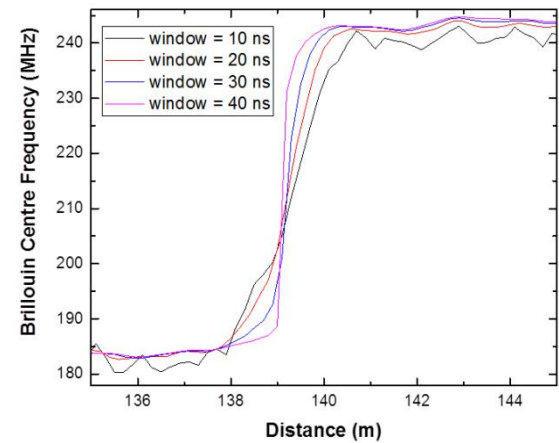


**Figure 8.** Experimental results of Brillouin centre frequency for 75°C temperature test with different window durations in the frequency transition region.

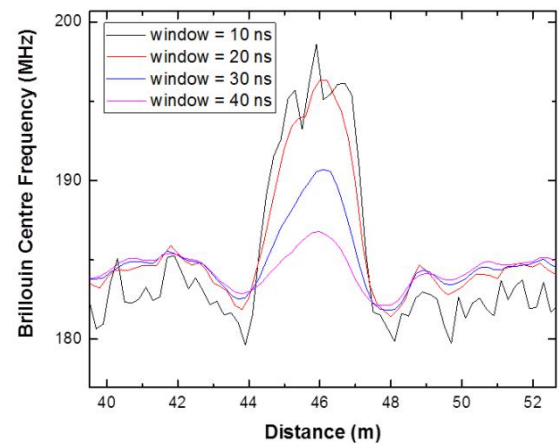


**Figure 9.** Experimental results of Brillouin centre frequency for 75°C temperature test with different window durations in the 0.5m section.

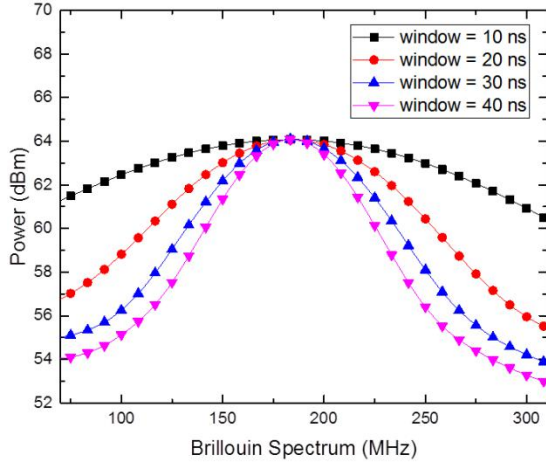


**Figure 10.** Experimental results of the Brillouin spectrum in a same position for the five durations of windows.

The reason for the low variation along the distance for the long window is due to more data involved in a window, which is equivalent to more times of averaging. In this case, 40 ns window provides four times more averaging than the 10 ns window. In the rising area, because of the low FWHM, the double peaks effect is easier to observe in the long window signal processing. In the results of short window, the double peaks are merged. Accordingly, long window has advantage to provide high measured frequency resolution. In the 0.5 m section detection, the 40 ns window did not show strength. 10ns window is more sensitive to the short event detection, which is due to short duration of time data averaging. Long window can bring low variation, but at the same time it losses some information. If the length of the event is less than the window duration, the measured frequency shift is always less than the real value, which is similar to the pulse length demonstrated in Ref (H. Zhang and Wu 2008). Moreover, long window can bring low FWHM, which indicate high frequency resolution to the STFT-BOTDR system. As a result, a long window can offer low variation, high spatial resolution and frequency resolution; a short window is more sensitive to strain or temperature events smaller than the pulse length detection.

#### 4. REFINEMENT ALGORITHM

The experimental results and physical explanation in section 3 demonstrate no window can be found for the STFT-BOTDR system to achieve high frequency resolution and small event detection simultaneously due to the time-frequency uncertainty principle. However, this paper utilised a combined window analysis algorithm to improve the system performance. In the signal processing, long rectangular window and short hamming window are applied. The rectangular window is longer than the probe pulse length; and the hamming window is shorter than the probe pulse

length. For example, if the probe pulse is 34 ns, the rectangular window can be chosen to be 40 ns and the hamming window has a length of 20 ns. The difference between Brillouin frequency shift results generated by two windows are experimentally illustrated in Fig. 11. In the temperature changing area (longer than the spatial resolution), the frequency difference has both positive and negative peaks shown in Fig. 12. However, in the shorter temperature event (such a 0.5 m section), the frequency difference only have negative peaks displayed in Fig. 13. Physically, the shorter windows can detect both the event longer or shorter than the spatial resolution, while the longer windows can only detect the event longer than the spatial resolution. Accordingly, the frequency difference between two kinds of window functions can be utilised as an indication whether the event section is longer or shorter than the spatial resolution. This window combination algorithm offers a rapid indication for small events happening along the fibre.

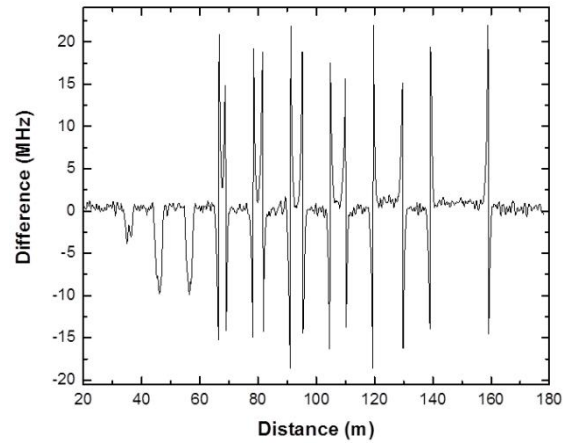


**Figure 11.** The difference between two Brillouin shifts for 40ns rectangular window windows and 10ns hamming window.

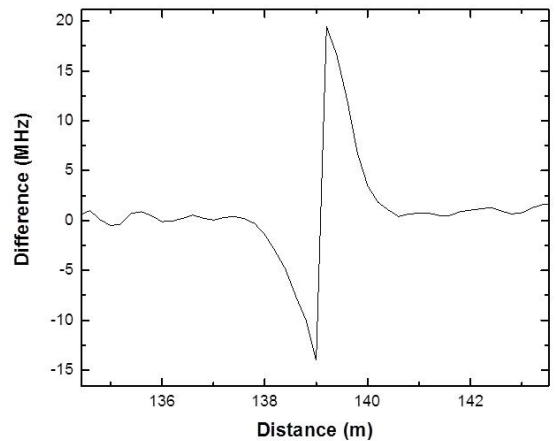


**Figure 12.** The difference between two Brillouin shift in the frequency changing area for 40ns rectangular window windows and 10ns hamming window.

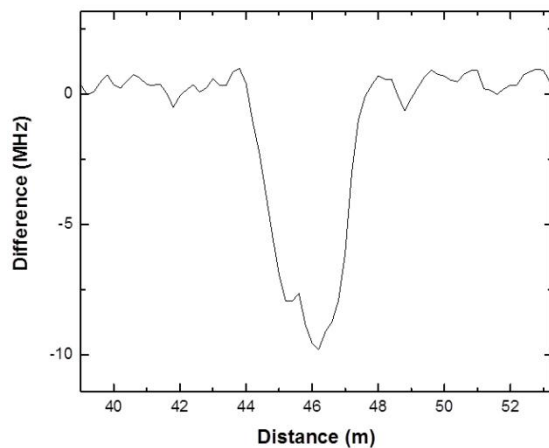


**Figure 13.** The difference between two Brillouin shift in the strain or temperature events smaller than the pulse length area for 40ns rectangular window windows and 10ns hamming window.

## 5. CONCLUSIONS

Five different types of window functions are utilised and experimentally compared in the STFT-BOTDR system in the paper. Long-window offers a better frequency resolution, while short-window offers a better performance for small event detection. Long and short windows can be combined together to enhance the capability of small event detection while keeping the same frequency resolution, indicating an optimised result from multiple windows analysis.

## ACKNOWLEDGEMENTS

Yifei Yu is supported by Schlumberger Foundation (Faculty for the Future). Linqing Luo and Bo Li are supported by the China Scholarship Council and Cambridge Commonwealth, European and International Trust.

## REFERENCE

- Abdelghani, Djebbari, and Bereksi Reguig Fethi. 2000. Short-Time Fourier Transform Analysis of the Phonocardiogram Signal. *IEEE* **9** (7803-6542): 844–47.
- Bao, Xiaoyi, and Liang Chen. 2011. Recent Progress in Brillouin Scattering Based Fiber Sensors. *Sensors (Basel, Switzerland)* **11** (4): 4152–87. doi:10.3390/s110404152.
- Busch, Paul, Teiko Heinonen, and Pekka Lahti. 2007. Heisenberg's Uncertainty Principle. *Physics Reports* **452** (6): 155–76. doi:10.1016/j.physrep.2007.05.006.
- Durak, Lütfiye, and Orhan Arikan. 2003. Short-Time Fourier Transform: Two Fundamental Properties and an Optimal Implementation. *IEEE Transactions on Signal Processing* **51** (5): 1231–42. doi:10.1109/TSP.2003.810293.
- Flandrin, Patrick, Yu-ting Lin, and Stephen McLaughlin. 2013. Time-Frequency Reassignment and Synchrosqueezing. *IEEE Signal Processing Magazine* **13** (1053-5888): 32–41.
- Geng, Jihong, Sean Staines, Mike Blake, and Shibin Jiang. 2007. Distributed Fiber Temperature and Strain Sensor Using Coherent Radio-Frequency Detection of Spontaneous Brillouin Scattering. *Applied Optics* **46** (23): 5928–32.
- Harris, F.J. 1978. On the Use of Windows for Harmonic Analysis with the Discrete Fourier Transform. *Proceedings of the IEEE* **66** (1): 51–83. doi:10.1109/PROC.1978.10837.
- Hlawatsch, Franz, and Auger Francois. 2008. *Time-Frequency Analysis Concepts and Methods*. ISTE Ltd and John Wiley & Sons, Inc.
- Horiguchi, Tsuneo, Kaoru Shimizu, Toshio Kurashima, Mitsuhiro Tateda, and Yahei Koyamada. 1995. Development of a Distributed Sensing Technique Using Brillouin Scattering. *Journal of Lightwave Technology* **13** (9512279): 1296–1302.
- Lee, Byounggho. 2003. "Review of the Present Status of Optical Fiber Sensors." *Optical Fiber Technology* **9** (2): 57–79. doi:10.1016/S1068-5200(02)00527-8.
- Lu, Yuangang, Rongrong Dou, and Xuping Zhang. 2008. Wideband Detection of Spontaneous Brillouin Scattering Spectrum in Brillouin Optical Time-Domain Reflectometry. In *2008 International Conference on Optical Instruments and Technology*, edited by Xuping Zhang, Wojtek J. Bock, Xiaoyi Bao, and Ping Shum, 7158:715818–715818 – 7. doi:10.1117/12.807012.
- Lu, Yuangang, Yuguo Yao, Xiaodong Zhao, Feng Wang, and Xuping Zhang. 2013. Influence of Non-Perfect Extinction Ratio of Electro-Optic Modulator on Signal-to-Noise Ratio of BOTDR. *Optics Communications*, no. **297** (June). Elsevier: 48–54. doi:10.1016/j.optcom.2013.01.080.
- Motil, Avi, Arik Bergman, and Moshe Tur. 2015. State of the Art of Brillouin Fiber-Optic Distributed Sensing. *Optics and Laser Technology* **78**. Elsevier: 1–23. doi:10.1016/j.optlastec.2015.09.013.
- Ohno, Hiroshige, Hiroshi Naruse, Mitsuru Kihara, and Akiyoshi Shimada. 2001. Industrial Applications of the BOTDR Optical Fiber Strain Sensor. *Optical Fiber Technology* **7**: 45–64.
- Wang, Feng, Xuping Zhang, Yuangang Lu, Rongrong Dou, and Xiaoyi Bao. 2009. Spatial Resolution Analysis for Discrete Fourier Transform-Based Brillouin Optical Time Domain Reflectometry. *Measurement Science and Technology* **20** (2): 025202. doi:10.1088/0957-0233/20/2/025202.
- Yu, Yifei, Linqing Luo, Li Bo, Linfeng Guo, Jize Yan, and Kenichi Soga. 2015. Double Peak-Induced Distance Error in Optical Time Domain Reflectometers Event Detection and the Recovery Method. *Applied Optics* **54** (28): 196–202.
- Zhang, Hao, and Zhishen Wu. 2008. Performance Evaluation of BOTDR-Based Distributed Fiber Optic Sensors for Crack Monitoring. *Structural Health Monitoring* **7** (2): 143–56. doi:10.1177/1475921708089745.